Eur. J. Biochem. 246, 373–379 (1997)

Viscoelasticity of actin-gelsolin networks in the presence of filamin

Wolfgang H. GOLDMANN[1], Markus TEMPEL[2], Irene SPRENGER[2], Gerhard ISENBERG[2] and Robert M. EZZELL[1]

[1] Surgery Research Labortories, Massachusetts General Hospital, Harvard Medical School Charlestown, USA
[2] Technical University of Munich, Biophysics, Garching, Germany

(Received 18 November 1996/20 February 1997) – EJB 96 1724/3

Cross-linking of actin filaments by filamin by means of frequency-dependent rheology yields an increase in the filament's elasticity and stiffness. Higher cross-linker (filamin) ratios are required for mean actin-filament lengths of 5–6 μm than for random-length distribution of actin filaments. The loss modulus (i.e. the viscous portion) in the region of the internal-chain dynamics [$G''(\omega) \approx \omega^{\alpha}$] is influenced by the cross-linking of filaments, and with an increasing molar ratio of filamin/actin a reduction of α is observed. Rheological measurements reveal that actin networks are already formed at the polymerizing stage at a molar ratio of filamin/actin of less than 1:100, and electron micrographs show phase separation of actin/filament networks of low density and of actin/filament bundles.

Keywords: viscoelasticity; actin network; filamin; gelsolin; rheology.

Filamin is an approximately 160-nm elongated, highly flexible homodimer of approximately 540 kDa, and is ubiquitous in mammalian cells [1, 2]. In its dimeric form, filamin has actin-binding sites at each amino-terminal end, and self-association sites at the carboxyl-terminal ends. This allows filamin to act as an efficient cross-linking protein in actin gels [3, 4]. Further, filamin is believed to be involved in connecting the cytoskeleton with the lipid membrane and β2-integrin [5–7].

Hou et al. [8] showed, in an extensive light-microscopic and fluorescence-photobleaching-recovery study, that filamin (at a low molar ratio of actin/filamin) bundles actin filaments, while at a high molar ratio the actin network remains isotropic. The molar ratio of filamin/actin that was critical for the shift from isotropic to network-bundle formation was 1:140. Further, Janmey et al. [9] reported that mixtures of actin filaments and filamin form gels that are physically equivalent to covalently cross-linked networks. The viscoelastic properties of filamin gels are similar to those of gels composed of avidin and biotinylated actin. Extensive rheological measurements have been carried out by Zaner [10] and Ruddies et al. [11], varying the actin concentration, the molar ratio of actin/filamin, and the frequency from 3×10^{-3} Hz to 0.5 Hz and from 1.8×10^{-3} Hz to 2.2 Hz, respectively. These researchers found that as the molar ratio of filamin increased, the plateau modulus G'_N, when measuring the elastic portion $G'(\omega)$ was increased, and the viscous portion, G'' ($= \omega\eta$), increased. Common to both studies was that the actin-length distribution was random, from 5 μm to 50 μm.

In the present study, we investigated the effect of actin filaments at a mean length (≈5–6 μm) on gels formed by filamin. We measured the dynamic moduli $G'(\omega)$ and $G''(\omega)$, which determine the elastic and viscous portion, and the creep (deformation) $J(t)$ and creep recovery $J_r(t)$ of gels, by means of a magnetically driven rotation disc rheometer. Further, we measured and examined actin-filamin networks at various molar ratios using electron microscopy.

MATERIALS AND METHODS

Protein preparation. Filamin was isolated by means of the method of Shizuta et al. [12]. Low-ionic strength-extraction of chicken gizzard was followed by Mg^{2+} and $(NH_4)_2SO_4$ precipitation, ion exchange, and gel-filtration column chromatography. For all experiments, a hydroxylapatite column was used to further purify the protein [13]. The purity of the filamin was determined by means of 7.5% SDS/PAGE following [14]. The concentration of purified filamin was measured by ultraviolet spectroscopy, using an extinction coefficient of 0.82 mg^{-1} cm^{-1} at 278.5 nm [15] according to the method of Bradford [16] with BSA as standard. A molecular mass of 270 kDa for monomeric filamin was used.

Actin was prepared according to procedures of Spudich and Watt [17], from acetone powder obtained from rabbit back muscle; this was followed by a gel-filtration step as described by MacLean-Fletcher and Pollard [18]. The biological activity of the purified actin was tested, by means of falling-ball viscometry, and its concentration was determined from its $A_{270\,nm}$ (absorbance coefficient = 0.63 mg^{-1} cm^{-1}). Fractionated G-actin was stored in 2 mM imidazole, pH 7.4, 0.2 mM $CaCl_2$, 0.5 mM ATP, 0.2 mM dithiothreitol and 0.005% NaN_3, for no longer than 10 days. For the polymerization studies in the rheometer, all proteins were added at the same time to 2 mM imidazole, pH 7.4, 50 mM KCl, 2 mM $MgCl_2$, 1 mM EGTA, 0.2 mM $CaCl_2$, 1 mM ATP.

Gelsolin was purified from bovine plasma serum by means of the procedure described by Cooper et al. [19]. The concentra-

Correspondence to W. H. Goldmann, Massachusetts General Hospital/Harvard Medical School Surgery Research Unit, Building 149, 13th Street Charlestown, MA 02129, USA
Fax: +1 617 726 5414.
E-mail: goldman@helix.mgh.harvard.edu

Abbreviations. $G'(\omega)$, dynamic modulus (elastic portion of the gel); $G''(\omega)$, loss modulus (viscous portion of the gel); G'_N, shear elastic constant; $|G^*|$, absolute value of the complex shear modulus; $J(t)$, creep (deformation); ω, frequency; φ, phase shift; η, viscosity; t, time; $\alpha(t)$, rotational amplitude; $G^*(\omega)$, viscoelastic impedance; $J_r(t)$, creep (deformation) recovery; ξ, mesh size of purely entangled actin network; r_{AG}, molar ratio of actin/gelsolin.

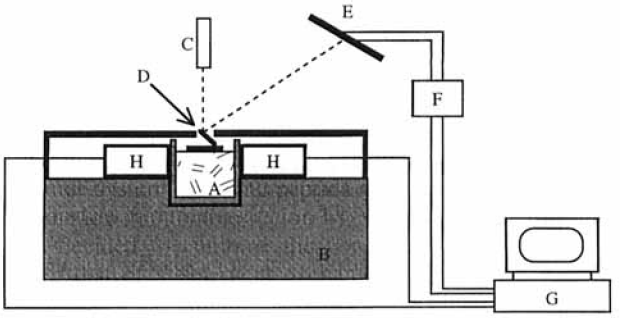

Fig. 1. Schematic diagram of the purpose-built oscillating rheometer. A, measuring quartz cuvette; B, aluminium block; C, laser; D, mirror attached to disc; E, photodiode; F, signal amplifier; G, computer. Two coils orientate the mirror (D) at a constant magnetic field, and two coils oscillate the disc (H) by a small amplitude of no more than 0.05. Components A, D and H are encaged by a metal chamber to shield off external magnetic fields.

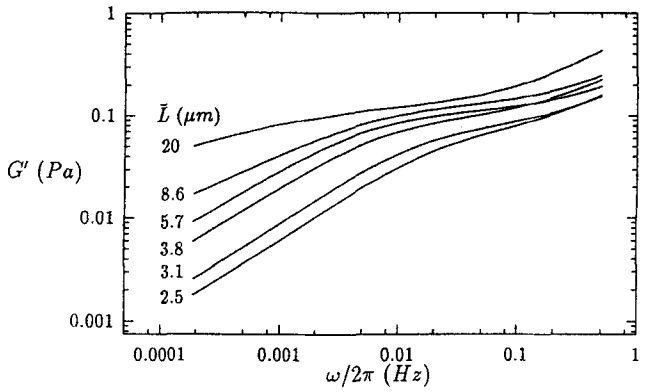

Fig. 2. Numerically transformed creep measurements [$J(t) \rightarrow G'(\omega)$] of 25 μM actin at various gelsolin molar ratios (r_{AG}). r_{AG} = 900–7400.

tion was determined by the Bradford method, with BSA as standard.

Rotation disc rheometer. The rotation disc rheometer has been described in detail by Müller et al. [20]. The storage (elastic) modulus $G'(\omega)$, loss (viscous) modulus $G''(\omega)$, and the creep (deformation) $J(t)$ were measured at $\omega/2\pi = 10^{-5}-10^{1}$ Hz and $t = 10^{-1}-10^{4}$ s. Using these dynamic moduli, the phase shift angle [$\tan(\varphi) = G''/G'$] was determined.

The rheometer consists of a cylindrical quartz cuvette with an inner diameter of 15 mm and a volume of about 1.5 ml. The base of the cuvette was mounted in an aluminum thermostated holder. A glass disc with a diameter of 8 mm was placed on the surface of the viscoelastic solution. Mounted on top of the disc were a magnet and deflection mirror with dimensions of $0.5\times0.5\times1.5$ mm^3 and 1.5×2.0 mm^2, respectively. The plane of the deflection mirror forms a 45° angle with the horizontal line. The quartz cuvette is surrounded by two perpendicularly oriented magnetic coils. One of these serves to fix the orientation of the disc, the other (the deflection coil) applies a shear force to the viscoelastic solution. When the dynamic moduli $G'(\omega)$ and $G''(\omega)$ are measured, the deflection coils are driven by an oscillatory voltage of frequency ω. In the present study, creep measurements [$J(t)$] were carried out at a constant voltage to these coils. The magnetic coils and the measuring cuvette were placed into a μ-metal chamber to shield the cuvette from external magnetic fields.

The rotational amplitude $\alpha(t)$ of the disc was analyzed as follows. The beam of a He-Ne-laser incident light was horizontally deflected by the mirror, in a parallel direction along the rotational axis of the disc. Its horizontal orientation was recorded by a position-sensitive photodiode, amplified and evaluated by computer.

The actin solution in the measuring cuvette was covered by a phospholipid monolayer (dimyristoylphosphatidylcholine), which is essential to avoid the gelation of actin owing to its denaturing at the air/water interface [19]. This ensures good mechanical contact with the glass disc when covered by a monolayer of octadecyltrichlorosilane. Protein mixtures of 400 μl were polymerized for about 15 h prior to rheometer experiments. A schematic view of the rotating disc rheometer is shown in Fig. 1.

Electron microscopy. Protein samples were absorbed to glow-discharged carbon-coated Formar films on copper grids for 60 s. The grids were washed with distilled water and excess fluid was removed by filter paper. Electron microcope grids were negatively stained with 0.8% uranyl acetate for 60 s.

Theoretical basis of the actin/gelsolin polymerization. The mathematical model of Coppin [21] was used to describe actin polymerization in the presence of gelsolin. This approach allows the prediction of the qualitative and quantitative distribution of the actin-filament length over time. Assuming that gelsolin blocks the barbed end of an actin filament, polymerization occurs only at the pointed end (k_+ 0.6 μmol^{-1} s^{-1} k_- 0.4 s^{-1}). We used 25 μM actin at various ratios of gelsolin to determine the filament length numerically (Fig. 2).

RESULTS

Frequency-dependent measurements. Prior to frequency measurements, 10 μM actin was polymerized in the presence of gelsolin at a molar ratio of 2000:1, to restrict the actin-filament contour length to 5–6 μm ([22, 32]; Fig. 2). Results of studies to determine the elastic portion [$G'(\omega)$] and the viscous portion [$G''(\omega)$] of the actin-gelsolin gel in the presence of filamin are shown in Fig. 3.

When measuring the elastic and viscous portions of the gel, in the presence and absence of filamin at a molar ratio of 300:1, (Fig. 3A) we observed no significant changes in the logarithmic plot. Thus, a relative increase in the plateau region (<0.1 Hz) of about 15% was calculated. When the molar ratio was changed to 100:1 (Fig. 3B) marked changes occurred. On examination of the plateau region, we determined a relative increase in $G'(\omega)$ and $G''(\omega)$ of about 60%. Ruddies et al. [11] reported an increase in viscoelastic parameters in the plateau region of greater than 100% in the absence of gelsolin. At a molar ratio of 50:1 (Fig. 3C), the viscoelastic changes were even more drastic; an increase by a factor of 4–5 was observed.

An aspect of filamin-actin cross-linking was detected at frequencies around 0.1 Hz, indicating internal-chain dynamics. In double-logarithmic plots, the slope of G' is constant, [$G'(\omega) \approx \omega^{0.50}$] at frequencies above 0.1 Hz, with the slope of G'' decreasing with increasing filamin concentration. An actin-gelsolin solution polymerizes at $G''(\omega) \approx (\omega^{\alpha})$ with $\alpha = 0.80$. Thus, in the presence of filamin at molar ratios of 300:1, 100:1 and 50:1, at α = 0,79, 0,68 and 0,45, respectively. The reduction of the ω dependence of the loss modulus G'' in the internal dynamic region could be explained by the high number of cross-linking points within the contour length of single filaments, which lower the energy dissipation.

This result is consistent with light-microscopic and rheologic observations of actin networks in the presence of talin. Kaufmann et al. [23] detected actin filaments with an average length of about 4 μm and 14 μm in the presence and absence of talin,

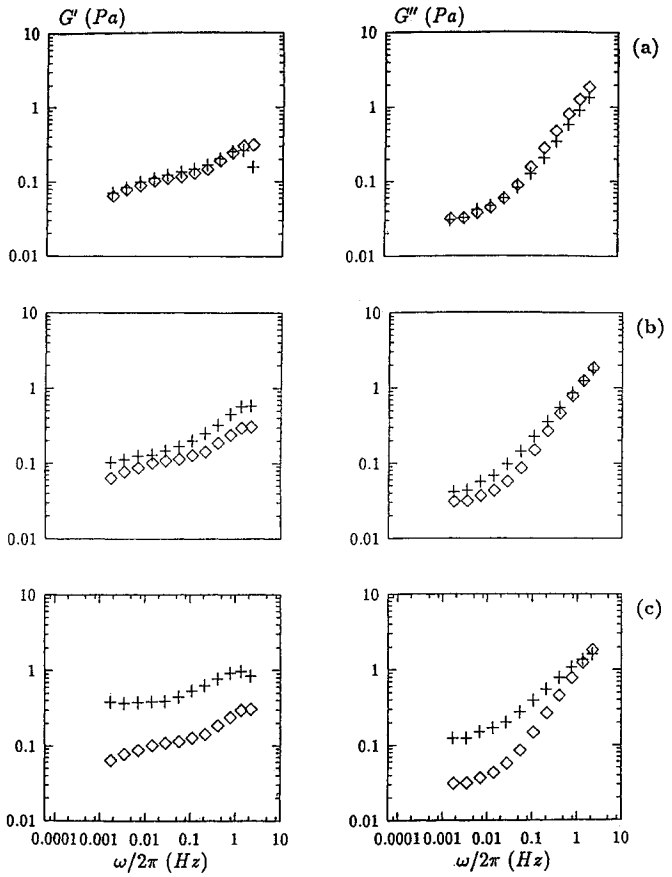

Fig. 3. Frequency measurements $G'(\omega)$ and $G''(\omega)$ of actin and gelsolin at different filamin concentrations. ◇, control experiments with 10 μM actin at a molar ratio to gelsolin of 2000:1. The molar ratios of actin/filamin (+) were 300:1 (A), 100:1 (B) and 50:1 (C). The logarithmic plot show relative changes of about 15% (A), about 60% (B) and by a factor of 4–5 (C).

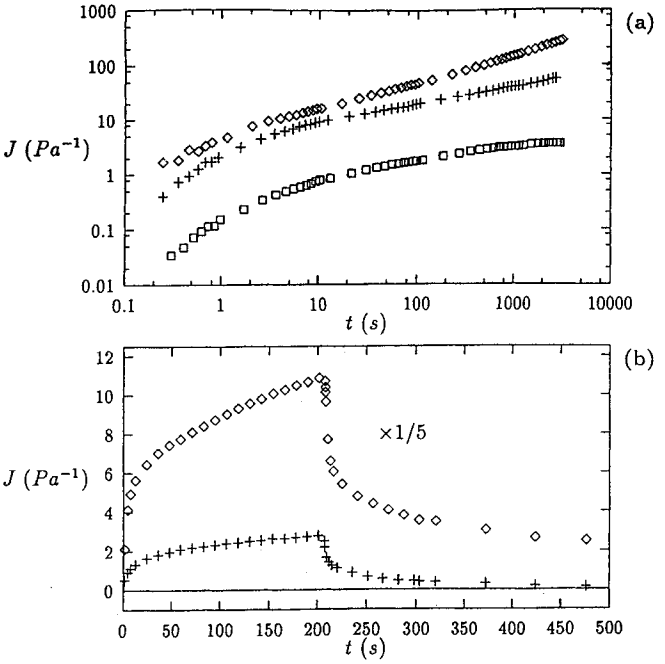

Fig. 4. Time dependence of the creep (deformation) of actin-filamin networks. The average contour length of actin was controlled by an actin to gelsolin molar ratio of 2000:1. (A) Double logarithmic plots of the $J(t)$ in the absence of filamin (◇) and in the presence filamin at actin/filamin molar ratios of 200:1 (+) and 40:1 (□). (B) Linear presentation of the $J(t)$ at less than 200 s and $J_r(t)$ at greater than 200 s in the absence of filamin (◇) and in the presence of filamin at an actin/filamin molar ratio of 50:1 (+). The *y*-axis scale is fivefold lower for results of experiments in the absence of filamin.

respectively. Ruddies et al. [24] reported that actin filaments in the presence of talin polymerize at $G''(\omega) \approx \omega^{0.80}$. Thus, the presence of talin caused a significant decrease in the effective segment length of actin filaments.

Creep measurements. Creep measurements were performed in the presence and absence of filamin to evaluate the time-dependent deformation of actin gels. The transient function $J(t)$ yields more reliable values for the viscoelasticity of actin networks at longer times than do the dynamic moduli $G'(\omega)$ and $G''(\omega)$. Fig. 4A shows examples of time-dependent measurements of the creep [$J(t)$] of pure actin and actin in the presence of filamin at molar ratios of 1:200 and 1:40. Results from these experiments indicate that the presence of filamin greatly reduces the creep. The cross-linking of actin filaments by filamin and the subsequent restriction of filament diffusion reduce the motility of actin filaments in the network. At high filamin concentrations, the mobility of actin filaments was limited insofar as the viscoelastic properties show macroscopic features similar to those of a solid state.

Another way to measure the viscoelastic properties of cross-linked polymers is by creep recovery [$J_r(t)$]. Fig. 4B shows pure actin and actin/filamin at a molar ratio of 1:50, for which the creep was measured for 200 s and then switched off. The recovery of the actin network in the presence of filamin was almost 100%, while in the absence of filamin it was less than 100%. The difference can be explained by the much greater ability of filamin cross-linked actin networks to retain elastic energy that is due to deformation, compared with pure actin networks. Such behavior can only be observed when the absolute deformation of networks is very small, i.e. when it is in the linear viscoelasticity range, which otherwise would lead to the disruption of the actin network [9].

Polymerization measurements. Measuring actin polymerization by various methods showed that the presence of filamin has little effect on the promotion of actin assembly [23, 24]. Hou et al. [8] observed, with 12–120 μM actin in the presence of filamin at a molar ratio of greater than 210:1, the formation of isotropic actin networks; at molar ratios of less than 140:1 anisotropic, laterally associated actin bundles were observed. We used rheology to verify these findings.

Polymerization of 3, 5 and 7 μM actin in the presence and absence of filamin at a constant molar ratio was performed in the rheometer. The viscoelastic parameters are described by the complex shear modulus $|G^*|$, which is a measure of the resistance of the solution versus the oscillatoric deformation characterized by its stiffness [27], and the phase shift φ, which indicates whether the gel is more viscous (φ approached $\pi/2$) or elastic (φ approaches 0). Fig. 5 shows the effect of filamin on actin polymerization. In the absence of filamin, a steady state was reached with increasing actin concentration. At 3 μM actin, the presence of filamin had little influence on $|G^*|$; however, at 5 μM and 7 μM actin, significant changes were observed. The time dependence of φ at 7 μM actin is particularly interesting at t less than 1000 s. A constant phase was observed with pure actin, and a continuously reduced phase was observed with actin in the presence of filamin. This was probably due to the mixture of actin networks and bundles, which form shortly after the on-

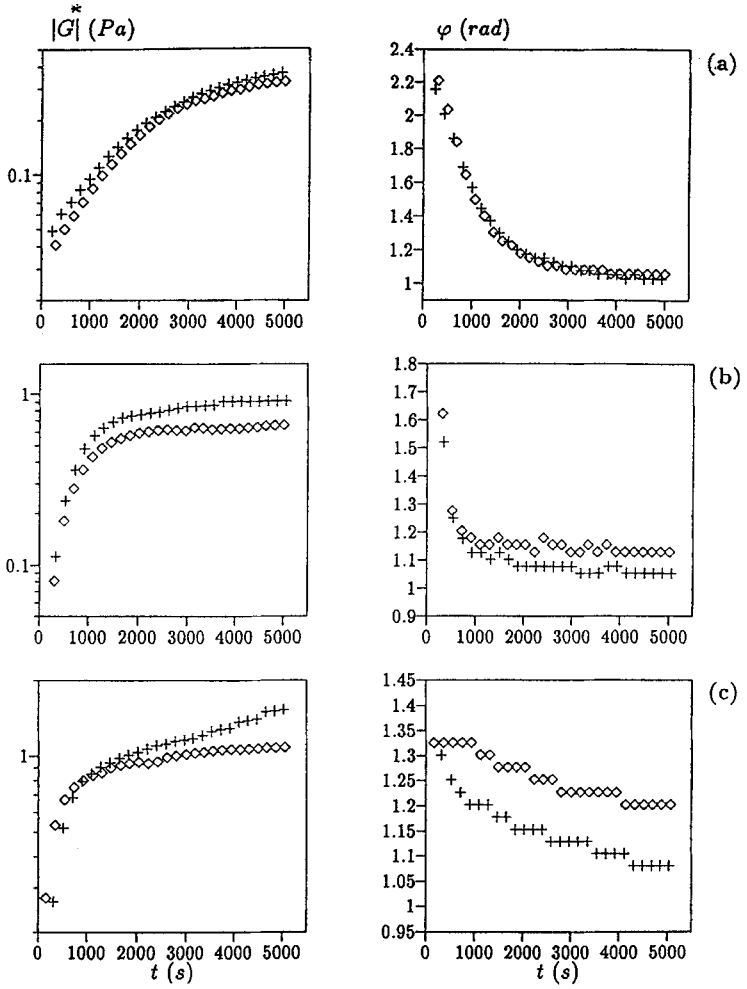

Fig. 5. Time dependence of $|G^*|$ and φ of actin polymerizing at different actin concentrations. Experiments were performed in the absence (◇) or presence (+) of filamin at molar ratios of actin/filamin of 100:1, at actin concentrations of 3 μM (A), 5 μM (B), and 7 μM (C). Only every fourth data point measured is shown.

set of polymerization. When the bundles were short, they had no influence on actin entanglement and, therefore, did not contribute to the viscosity of the solution. With progressing polymerization, however, the length of filament bundles grow and start to cross-link, building a network which is likely to be stiffer than a network of single filaments. This might explain why the stiffness of actin solutions in the presence of filamin increased over longer periods of time ($t > 1000$ s).

Electron microscopy. Electron microscopy was used to examine the microstructural change in the actin-filament network caused by filamin. Three images of the same actin-gelsolin concentration, and at actin/filamin ratios of 300:1 and 20:1, and in the absence of filamin are shown in Fig. 6.

Fig. 6A shows that there is little change in the organization of the actin network compared with the control. Only a few density fluctuations of the network were observed, which are indicative of microgel formation [28, 29]. At low filamin concentrations, signs of actin-bundle formation were found. This changed dramatically at high filamin concentrations Fig. 6B. In addition to an actin network of low spatial density, a macroscopic network of actin bundles could be recognized.

DISCUSSION

The actin network provides a versatile model with which to study the fundamental properties of gels. In a living cell, a large number of structural and regulatory actin proteins exist, enabling the cell to modify its network and control its shape and motility. These proteins include filamin and gelsolin, each of which interacts with actin in its own way. It is possible that the ability of filamin to cross-link actin filaments allows the cell to resist deformation, and that the small amounts of gelsolin in cells very subtly regulate the polymerization of actin. An important factor in these processes is that most components seem to attach with a low affinity, which normally does not exceed K_d values of 1 μM at ambient temperature [13]. Thus, by employing a multitude of components that interact with modest affinities, the cell gains a high degree of viscoelasticity.

Here we studied filamin and gelsolin to examine changes in the viscoelastic behavior of actin filaments of constant mean length. These results were compared with previous findings of Zaner [10], and Ruddies et al. [11] of random-length actin filaments cross-linked with filamin. Actin filaments of random length form heterogeneous gels, which consist of clusters of cross-linked short chains that are interconnected by long chains. Tempel et al. [30] described this structure as the consequence of the slow generation of actin trimers, which act as nuclei for the polymerization process. It leads to the initial formation of very long chains, which cannot effectively entangle due to their semiflexibility. Subsequently, shorter chains form that are cross-linked among themselves and coupled to long chains. Because of the fast diffusion of short chains, the gelation is associated

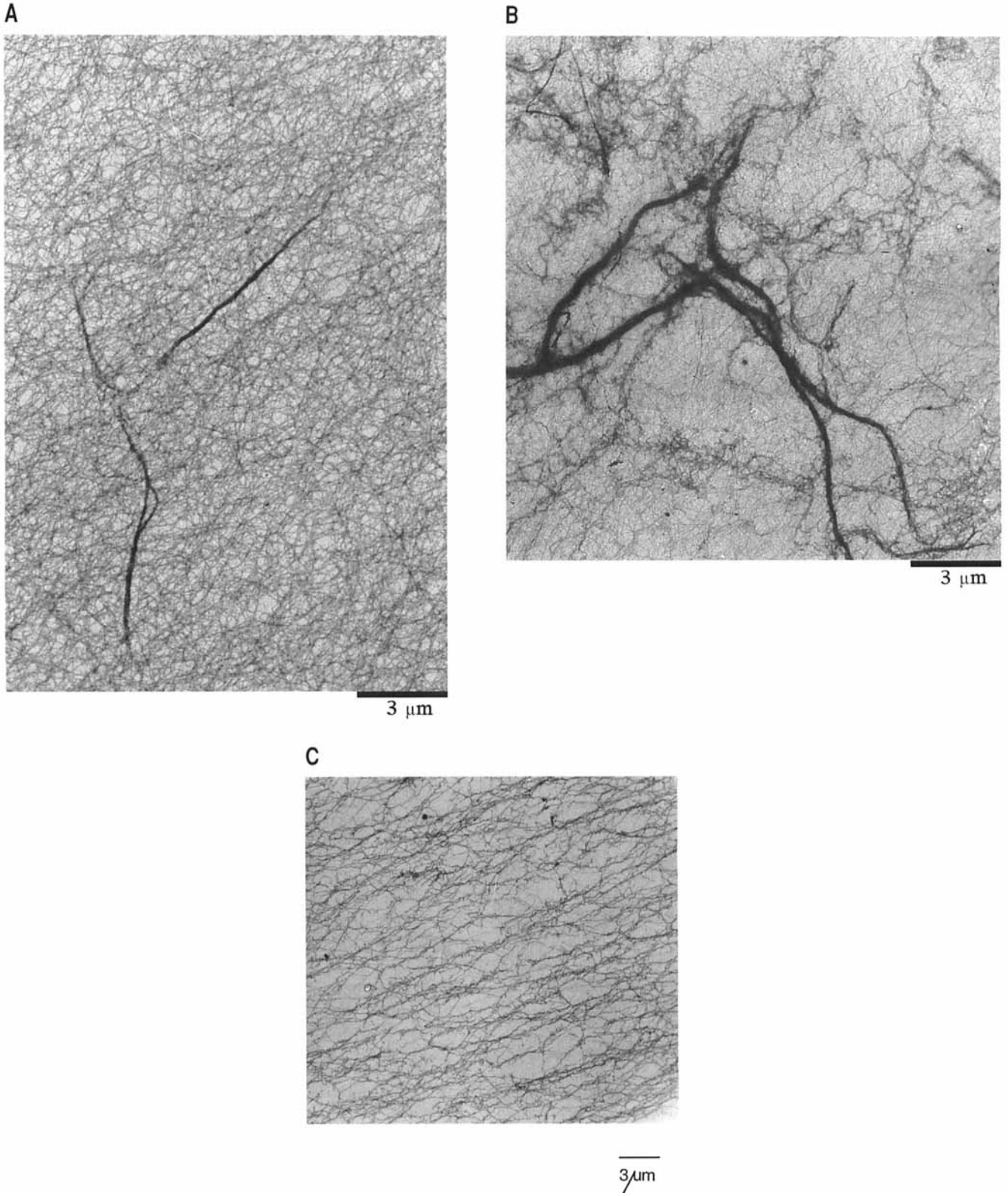

Fig. 6. Negative-staining electron micrographs of actin-filamin networks in the presence of gelsolin. 10 μM actin in the presence of gelsolin (2000:1) at a molar ratio to filamin of 300:1 (A), 20:1 (B), and in the absence of filamin (C). Bar = 3 μm.

with local phase separation. A microgel composed of clusters of interconnected short chains coupled by long filaments results, which can be characterized by the size of the mesh. Electron micrographs (Fig. 6) indicate that the gel is a homogeneous network at a low molar ratio of filamin cross-linking. Regions of more densely packed and highly cross-linked actin filaments increase with higher filamin concentration, and at a very high degree of cross-linking complete separation into bundle structures and dilute solution of residual filaments occur.

The present study shows that the gelation of networks of semiflexible actin filaments passes through the same sequence of transitions as do synthetic gels at increasing degree of cross-

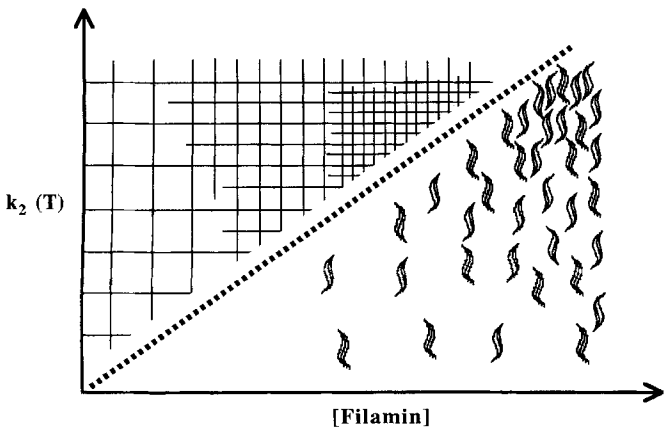

Fig. 7. Hypothetical phase diagram of actin-filamin networks based on kinetic measurements. The abscissa represents increasing filamin concentration at constant actin/gelsolin molar ratio, and the ordinate the rate of crosslinking/bundling [k_2] of the actin-filamin complex [33]. The dividing line depicts the imaginary phase boundary between the solid and gel state. With increasing temperture, k_2 and, subsequently, the crosslinking/bundling activity increase. With increasing [filamin] at constant [actin] a tighter actin-filamin network is observed.

linking [31]. Since bundle formation is also induced by another actin cross-linker, α-actinin [30, 32], we believe that this behavior observed with filamin might account for actin-cross-linking proteins in general (Fig. 7). As the dissociation/association equilibrium of an actin/filamin system easily shifts to the side of association by adjusting the fraction of polymerizable actin [33, 34], the sensitive dependence of the gel point on the actin concentration and on the actin-filamin ratio provides the cell with a mechanism to regulate its shape and movement. Further, it is possible that several other actin-binding proteins affect the viscoelasticity of actin gels, but evidence that these proteins influence the mechanics of cells has been shown in only a few cases [35–37]. Using a rheometer over a wide frequency range (>50 Hz) could help to define the role of actin-binding proteins, by providing information on the elastic modulus or response of the cell to the applied shear, i.e. the cell's dynamic energy (G'), the viscous modulus (G''), i.e. the cell's stored energy, and the creep [$J(t)$], i.e. the cell's elastic energy over a period of time, or its ability to sustain stresses. This non-invasive method has some advantages in that the shear strain imposed is unlikely to damage the cell, and the viscoelastic response is due to deformation of a collective cell mass rather than of individual cells, as is the case with atomic force microscopy [35].

We thank Ms. Hulda Kirpal and Ms. Karin Scharpf, for protein purification, and Zeno Guttenberg, for the graphs. We are grateful for discussions with Drs P. A. Janmey and E. Sackmann. We thank Ms. Judith Feldmann for careful reading of this manuscript. This work was financially supported by the *Deutsche Forschungsgemeinschaft* (to WHG and GI), American Cancer Society (to RME) and North Atlantic Treaty Organization (to WHG and RME).

REFERENCES

1. Hartwig, J. H. & Stossel, T. P. (1975) Isolation and properties of actin, myosin, and a new actin-binding protein in rabbit alveolar macrophages, *J. Biol. Chem. 250*, 5696–5705.
2. Hartwig, J. H. & Stossel, T. P. (1981) The structure of actin binding protein molecules in solution and interacting with actin filaments *J. Mol. Biol. 145*, 563–581.
3. Nunnally, M. H., Powell, L. D. & Craig, S. W. (1981) Reconstitution and regulation of actin gelsol transformation with purified filamin and villin, *J. Biol. Chem. 256*, 2083–2086.
4. Cortese, J. D. & Frieden, C. (1990) Effect of filamin and controlled linear shear on the microheterogeneity of F-actin/gelsolin gels, *Cell Motil. Cytoskeleton 17*, 236–249.
5. Tempel, M., Goldmann, W. H. & Isenberg, G. (1994) Computer analyses suggest interactions of non-muscle filamin with lipid membranes, *FEBS Lett. 350*, 169–172.
6. Tempel, M., Goldmann, W. H., Dietrich, C., Niggli, V., Weber, T., Sackmann, E. & Isenberg, G. (1994) Insertion of filamin into lipid membranes examined by calorimetric, film balance and lipid labeling method, *Biochemistry 33*, 12565–12572.
7. Sharma, C. P., Ezzell, R. M. & Arnaout, M. A. (1995) Direct interaction of fialmin (ABP-280) with the beta2-integrin subunit CD18, *J. Immunol. 154*, 3461–3470.
8. Hou, L., Luby-Phelps, K. & Lanni, F. (1990) Brownian motion of inert tracer macromolecules in polymerized and spontaneously bundled mixtures of actin and filamin, *J. Cell Biol. 110*, 1645–1654.
9. Janmey, P. A., Hvidt, S., Lamb, J. & Stossel, T. P. (1990) Resemblance of actin-binding protein/actin gels to covalently crosslinked networks, *Nature 345*, 89–92.
10. Zaner, K. S. (1986) The effect of the 540-kilodalton actin crosslinking protein, actin-binding protein, on the mechanical properties of F-actin, *J. Biol. Chem. 261*, 7615–7620.
11. Ruddies, R., Goldmann, W. H., Isenberg, G. & Sackmann, E. (1993) The viscoelastic moduli of actin/filamin solutions: A micro-rheologic study, *Biochem Soc. Trans. 21*, 37S.
12. Shizuta, Y., Shizuta, H., Gallo, M., Davies, P. & Pastan, I. (1976) Purification and properties of filamin, an actin-binding protein from chicken gizzard, *J. Biol. Chem. 251*, 6562–6567.
13. Goldmann, W. H. & Isenberg, G. (1993) Analysis of filamin and α-actinin binding to actin by stopped flow method, *FEBS Lett. 336*, 408–410.
14. Laemmli, U. K. (1970) Cleavage of structural proteins during the assembly of the head of bacteriophage T4, *Nature 227*, 680–685.
15. Koteliansky, V. E., Glukhova, M. A., Shirinsky, V. P., Smirnov, V. N., Bushueva, T. L., Filimonov, V. V. & Venyaminow, S. W. (1982) A structural study of filamin, a high-molecular-weight actin-binding protein from chicken gizzard, *Eur. J. Biochem. 121*, 553–559.
16. Bradford, M. M. (1976) A rapid and sensitive method for the quantitation of microgram quantities of protein utilizing the principle of protein-dye binding, *Anal. Biochem. 72*, 248–254.
17. Spudich, J. A. & Watt, S. (1971) The regulation of rabbit skeletal muscle contraction. I. Biochemical studies of the interaction of the tropomyosin-troponin complex with actin and the proteolytic fragments of myosin, *J. Biol. Chem. 246*, 4866–4871.
18. MacLean-Fletcher, S. D. & Pollard, T. D. (1980) Viscosimetric analysis of the gelation of Acanthamoeba extracts and purification of two gelation factors, *J. Cell Biol. 85*, 414–428.
19. Cooper, J. A., Bryan, J., Schwab, I. B., Frieden, C., Loftus, D. J. & Elson, E. L. (1987) Microinjection of gelsolin into living cells, *J. Cell Biol. 104*, 491–501.
20. Mueller, O., Gaub, H. E., Baermann, M. & Sackmann, E. (1991) Viscoelastic moduli of sterically and chemically cross-linked actin networks in the dilute to semidilute regime: measurements by an oscillating disk rheometer, *Macromolecules 24*, 3111–3120.
21. Schmidt, C. F., Baermann, M., Isenberg, G. & Sackmann, E. (1989) Chain dynamics, mesh size, and diffusive transport in networks of polymerized actin. A quasielastic light scattering and microfluorescence study, *Macromolecules 22*, 3638–3649.
22. Coppin, C. M. & Leavis, P. C. (1992) Quantitation of liquid-crystalline ordering in F-actin solutions, *Biophys. J. 63*, 794–807.
23. Kaufmann, S., Kaes, J., Goldmann, W. H., Sackmann, E. & Isenberg, G. (1992) Talin anchors and nucleates actin filaments at lipid membranes: a direct demonstration, *FEBS Lett. 314*, 203–205.
24. Ruddies, R., Goldmann, W. H., Isenberg, G. & Sackmann, E. (1993) The viscoelasticity of entangled networks: the influence of defects and the modulation by talin and vinculin, *Eur. Biophys. J. 22*, 309–321.
25. Stossel, T. P., Chaponnier, C., Ezzell, R. M., Hartwig, J. H., Janmey, P. A., Kwiatkowski, D. J., Lind, S. E., Smith, D. B., Southwick, F. S., Yin, H. L. & Zaner, K. S. (1985) Nonmuscle actin-binding proteins, *Annu. Rev. Cell Biol. 1*, 353–402.

26. Senger, R. & Goldmann, W. H. (1995) The influence of cations and ionic strength on actin polymerization in the presence/absence of α-actinin, *Biochem. Mol. Biol. Int. 35*, 103–109.
27. Wachsstock, D. H., Schwartz, W. H. & Pollard, T. D. (1993) Affinity of alpha-actinin for actin determines the structure and mechanical properties of actin filament gels, *Biophys. J. 65*, 205–214.
28. Sackmann, E. (1994) Intracellular and extracellular macromolecular networks – physics and biological function, *Macromol. Chem. Phys. 194*, 7–28.
29. Sackmann, E. (1994) Membrane bending energy concept of vesicle- and cell-shapes and shape-transitions, *FEBS Lett. 346*, 3–16.
30. Tempel, M., Isenberg, G. & Sackmann, E. (1996) Temperature induced sol-gel transition and microgel formation in α-actinin cross-linked actin networks: a rheological study, *Phys. Rev. E54*, 1802–1810.
31. deGennes, P. G. (1979) *Scaling concepts in polymer physics*, Cornell University Press, Ithaka.
32. Wachsstock, D. H., Schwartz, W. H. & Pollard, T. D. (1994) Cross-linker dynamics determine the mechanical properties of actin gels, *Biophys. J. 66*, 801–809.
33. Goldmann, W. H., Senger, R. & Isenberg, G. (1994) Analysis of filamin-actin binding and cross-linking/bundling by kinetic method, *Biochem. Biophys. Res. Commun. 203*, 338–343.
34. Senger, R., Goldmann, W. H. & Isenberg, G. (1994) The influence of cations on the polymerization of actin and actin in the presence of α-actinin/filamin, *Biochem. Soc. Trans. 22*, 57S.
35. Goldmann, W. H. & Ezzell, R. M. (1996) Viscoelasticity in wild-type and vinculin-deficient (5.51) mouse F9 embryonic carcinoma cells examined by atomic force microscopy and rheology, *Exp. Cell Res. 226*, 234–237.
36. Eichinger, L., Koeppel, B., Noegel, A. A., Schleicher, M., Schliwa, M., Weijer, K., Wittke, W. & Janmey, P. A. (1996) Mechanical perturbation elicits a phenotypic difference between Dictyostelium wild-type cells and cytoskeletal mutants, *Biophys. J. 70*, 1054–1060.
37. Malek, A. M. & Izumo, S. (1996) Mechanism of endothelial cell shape change and cytoskeletal remodeling in response to fluid shear stress, *J. Cell Sci. 109*, 713–726.